Journal of Environmental Radioactivity 222 (2020) 106325

Contents lists available at ScienceDirect

Journal of Environmental Radioactivity

journal homepage: http://www.elsevier.com/locate/jenvrad

Spatial distribution, risk assessment and influence factors of terrestrial gamma radiation dose in China

Wenli Feng [a,b,c,*], Yongfang Zhang [a,**], Yunlin Li [a,c], Ping Wang [a,c], Chaosheng Zhu [a,c], Lei Shi [d], Xiaonan Hou [a], Xiaoping Qie [a]

[a] School of Chemistry and Chemical Engineering, Zhoukou Normal University, Zhoukou, 466001, China
[b] Henan Key Laboratory of Rare Earth Functional Materials; The Key Laboratory of Rare Earth Functional Materials and Applications, Zhoukou Normal University, Zhoukou, 466001, China
[c] Zhoukou Key Laboratory of Environmental Pollution Control and Remediation, Zhoukou Normal University, Zhoukou, 466001, China
[d] School of Resources and Environmental Engineering, Henan University of Engineering, Zhengzhou, 451191, China

ARTICLE INFO

Keywords:
Terrestrial gamma radiation
Spatial interpolation
Mapping
Risk assessment

ABSTRACT

The current spatial distribution of the risk of terrestrial gamma radiation in China were investigated by using spatial interpolation. And the driving factors influence on the terrestrial gamma radiation dose (TGRD) distribution were identified using the geographic detector, a new statistical method based on the nonlinear hypothesis. The results showed that the values of TGRD were range from 60 to 195 nGy h^{-1} with the average of 86.5 nGy h^{-1}, and the higher values were recorded in Qingahi–Tibet Plateau, which were all within the range of background value in China. In addition, the radiological indices, ELCR (Excess Lifetime Cancer Risk), TGRD and AEDE (Annual Effective Dose Equivalent) were also within the acceptable range of values by risk assessment. The results by use of the geographic detector showed that sunshine duration, atmosphere pressure, altitude, and rainfall condition have closely related to the TGRD distribution. In addition, these meteorological factors and altitude had more impact on TGRD than the air pollution-related factors. Our study can provide useful information on studying the influence mechanism of the TGRD distribution, the variability of the natural terrestrial gamma radiation in China, and exposure data for risk assessment from low dose chronic exposures.

1. Introduction

Inevitably, human beings are continuously exposed to the natural radiation, 84% of this comes from terrestrial, and 16% from cosmic sources (UNSCEAR, 2000). Terrestrial gamma radiation dose (TGRD) plays an important role in assessing the natural radiation, because it can be used as a comprehensive index, and reflect the true level of natural radiation (Al-Ghorabie, 2005; Tufail et al., 2006; Alomari et al., 2019). Additionally, terrestrial gamma dose rate can predict the radon flux or potential geogenic radon (Manohar et al., 2013; Torres et al., 2018). Although natural radiation exist in low doses in our environment, significant gamma radiation exposure may constitute potential risk for human health because of the long term exposure situation (Jibiri, 2001). Therefore, studies of natural radiation deserve to be conducted.

To date, there are many studies have reported the spatial distribution of TGRD and the assessment of related health risk in some countries and regions. The results of these studies focused on the specific areas, such as the uranium mines (Momčilović et al., 2010; Sethy et al., 2014), riparian and coastal areas (Sharma et al., 2014; El Zrelli et al., 2019). Moreover, because of the increasing social concern, previous work studied the external irradiation by gamma radiation emitted by building materials with a mineral component, containing natural radionuclides from the U-238 series, the Th-232 series and K-40 (Ravisankar et al., 2016; Kumara et al., 2018; Ouakarrouch et al., 2019; Smetsers and Tomas, 2019; Kuang et al., 2020). Overall, these building materials are made of the natural materials, such as rock, sand, clay, etc, which also contain a certain amount of radionuclide. Thus, the radioactivity level of building materials are close related to the geochemical characteristics of natural materials (Lu et al., 2014). Assessment of natural radiation in the building materials or land areas usually using the hazards index methods. Health risk related indices including internal hazards index (H_{int}), external hazard index (H_{ext}), the effective dose rate (AEDE) and

* Corresponding author. School of Chemistry and Chemical Engineering, Zhoukou Normal University, Zhoukou, 466001, China.
** Corresponding author. School of Chemistry and Chemical Engineering, Zhoukou Normal University, Zhoukou, 466001, China.
E-mail addresses: fwlandy@csu.edu.cn (W. Feng), yfzhang1988@126.com (Y. Zhang).

https://doi.org/10.1016/j.jenvrad.2020.106325
Received 27 February 2020; Received in revised form 1 June 2020; Accepted 1 June 2020
Available online 17 June 2020

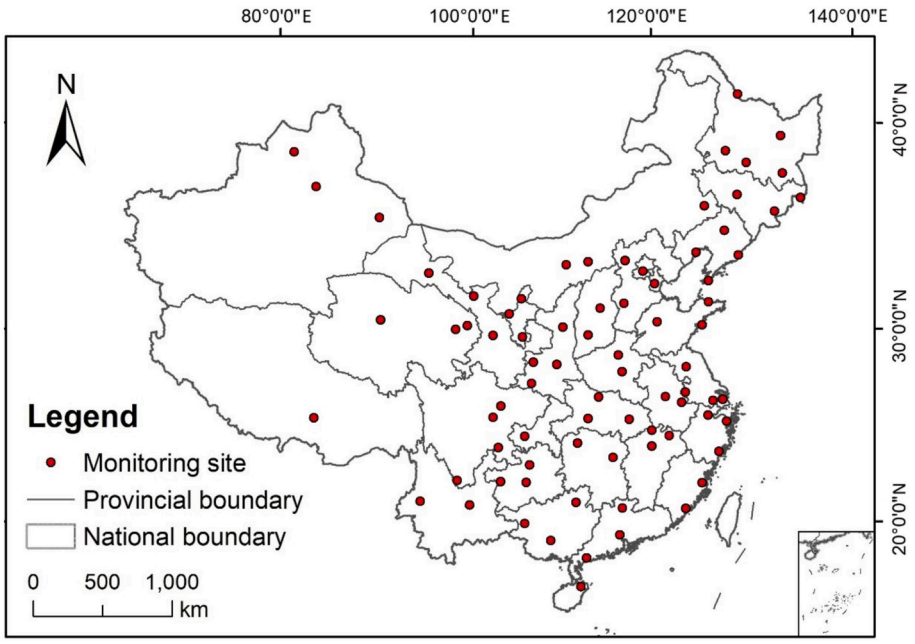

Fig. 1. The distribution of monitoring sites in China.

the excess lifetime cancer risk (ELCR), which were calculated in many references (Sethy et al., 2014; Alazemi et al., 2016; Belyaeva et al., 2019; Monica et al., 2019). However, the future study on health risk assessment of natural radiation should be concerned the health effect of long-term exposure to low doses.

Previous studies showed that terrestrial gamma radiation was strongly dependent on the composition of the soil and the rocks and the radionuclides contained within them (Momčilović et al., 2010; Sanusi et al., 2014). Actually, many environmental variations changes in space and time can also impact the natural radiation level (Abba et al., 2017; Szabó et al., 2017; Yeşilkanat et al., 2017; Torres et al., 2018). For instance, many studies showed that the rainfall or snowfall could seriously influence the environmental gamma radiation. This mainly because of the atmospheric radon daughters were scavenged, and reached to the ground, which was dubbed "radon washout", and that could significantly increase temporarily the environmental gamma radiation. Sometimes, it can increase gamma radiation by tens and even hundreds percent (Nishikawa et al., 1995; Mercier et al., 2009; Yakovleva et al., 2016). However, the impact of the environmental factors, such as the variations of meteorological indices and air pollution indices, on the radiation level are still unclear.

There are many different geographical regions in China as well as various types of climate. These various conditions can cause the changes of the terrestrial gamma radiation. There were total 79 sites sampled in National Radiation Environmental Monitoring System of China, which had been established to cover all province in mainland. The dynamic

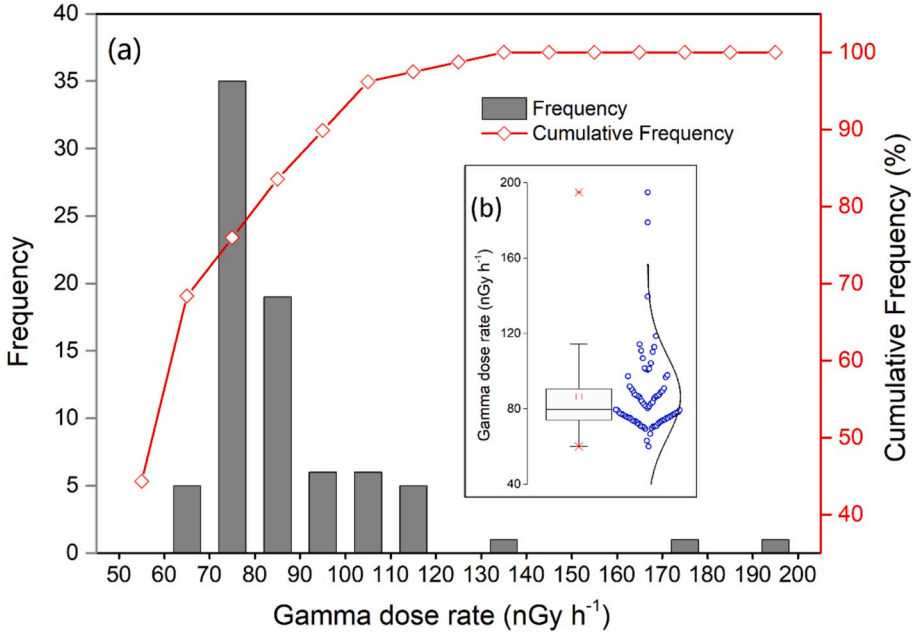

Fig. 2. Statistical analysis of terrestrial gamma radiation dose rates measured at 1 m above the ground surface (n = 79 × 12). Pareto chart (a), box plot and scatterplot (b) showing the showing the distributions of TGDR in China.

data and the quarterly bulletin were also released online regularly by the system. Of that, the gamma radiation contains the natural radionuclides of Th-232, Ra-226, and K-40. The main aims of this study are to (1) describe the spatial distribution of TGRD in China using the interpolation method, (2) perform the evaluation of natural radioactivity levels in China, and (3) investigate the influencing factors driving the difference of spatial distribution of TGRD. The findings of this study are helpful in indicating the current situation of gamma radiation level and in assessing the associated radiation hazard to population health. Furthermore, these can also fill the gap of the study on driving mechanisms of geographical discrepancy of TGRD.

2. Methods and materials

2.1. Study area and data sources

As shown in Fig. 1, there are total of 79 monitoring sites distribute in different cities provinces of China mainland. The TGRD was measured at the 1 m above the ground, and the results were published on the national radiation environmental data evaluation system. In this study, the data of gamma dose rate were collected from the quarterly bulletin released by National Radiation Environmental Data Evaluation System (MEP, 2018). The prepared influence factors were used mainly include the meteorological factors, air quality and geographic factors. The meteorological data included rainfall, air temperature, atmosphere and vapour pressure, relative humidity, wind speed, and sunshine duration were provided by the National Meteorological Data Center (CMA, 2018). The air quality data were collected from the China National Environmental Monitoring Center (CNEMC, 2018; Feng et al., 2019a). The altitude data of monitoring sites were obtained on the National Tibetan Plateau Data Center. We selected 30 monitoring sites in 30 capital cities as the study objectives, because of the meteorological data could not be obtained in some small and medium cities.

2.2. Assessment method

The annual effective dose equivalent (AEDE), in mSv y^{-1}, which represents effective dose equivalent to population from terrestrial gamma radiation, is estimated using the following equation (SEPA, 1993; Alazemi et al., 2016):

$$AEDE = TGRD \times DCF \times OF \times T \times 10^{-6} \quad (1)$$

where, the TGRD is terrestrial gamma radiation dose rate (nGy h^{-1}) for the measured samples were determined from the specific activity concentration, in addition to the associated radiological risks from the absorbed dose at 1 m above the ground surface (UNSCEAR, 2000; Alazemi et al., 2016); DCF is dose conversion factor, which is equal to 0.7 Sv Gy^{-1} for adults (UNSCEAR, 2000); OF is outdoor occupancy factor (20%), and T is the time to convert from year to hour (8760 h y^{-1}).

The excess lifetime cancer risk (ELCR) represents the probability of cancer incidence in a human population for a specific lifetime from the exposure to natural radiation (Taskin et al., 2009). The ELCR was calculated using the equation:

$$ELCR = AEDE \times DL \times RF \quad (2)$$

where DL is duration of life, 77 years, according to the gazette released by the National Health Commission of China in 2019 (NHC, 2019; Feng et al., 2019b), and RF is risk factor, which represents fatal cancer risk per Sievert. For stochastic effects, the value of 0.05 Sv^{-1} for public (ICRP, 2008). In this work, the calculated results were compared with results reported from the rest urban areas of the world.

2.3. Statistical analysis

In order to further identify the critical factors influenced the distribution of gamma dose rate, the geographic detector method is used to identify those from potential influencing factors (Wang et al., 2010). The geographic detector is a new statistical method with the nonlinear hypothesis to measure spatial stratified heterogeneity and detect explanatory factors and analyze the interactive relationship among variables, which has been widely used in many fields of natural and social sciences (Ren et al., 2014; Luo et al., 2016; Wang et al., 2016; Wei et al., 2020; Zhang et al., 2020). The geographic detector included four modules, which are the risk detector, factor detector, ecological detector and interaction detector (Wang et al., 2016; Bai et al., 2019). In this study, the factor detector was used, which could examine the determinant

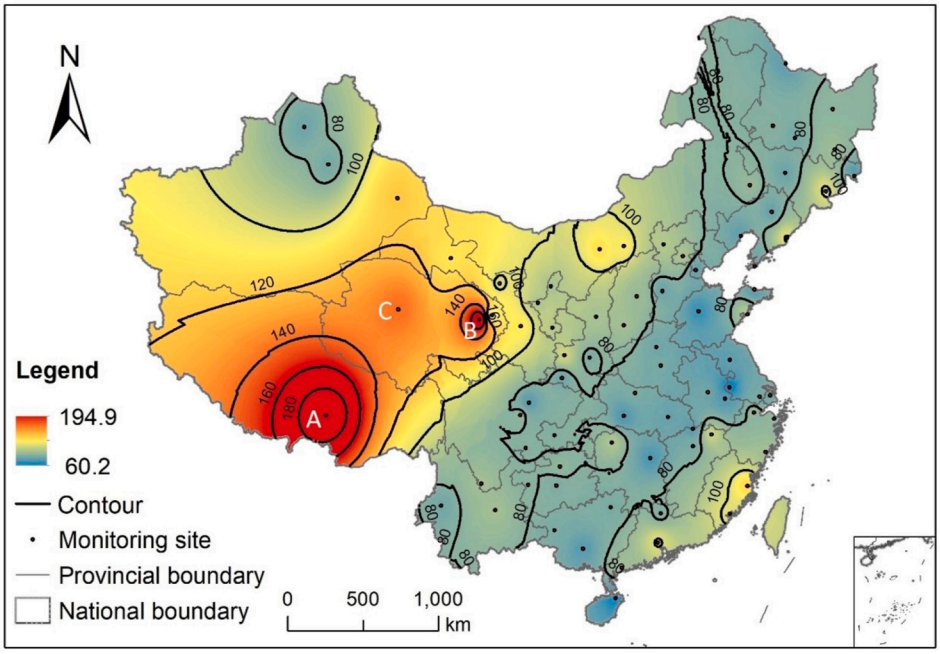

Fig. 3. Isodose map of the outdoor terrestrial gamma radiation dose rate in China. (A, B and C were the sampling sites with the high values in the Qinghai–Tibet Plateau).

power of driving factors (*Xs*) to *Y* by the *q* statistic value. The gamma dose rate was *Y*, and the input data (*Xs*) were meteorological data, air quality and geographic data. The *q* value was calculated using Eq. (3) (Wang et al., 2010):

$$q = 1 - \frac{1}{N\sigma^2}\sum_{i=1}^{L} N_i\sigma_i^2 \quad (3)$$

where q is the determinant power of the risk factor and the determinant power of heterogeneity of target variables, with range from 0 to 1, the larger the q value, the greater is the influence of the index on the variables (Wei et al., 2020). The σ denotes the variance of gamma dose rates of the study area. The i = 1, 2, …, L is stratification of impact factor *X* (Wang and Hu, 2012).

For visualization of the spatial distribution of terrestrial gamma radiation dose rate, the sites distribution and isodose map were generated by using the ArcGIS software (version 10.2). The Inverse Distance Weighting (IDW) method was conducted for interpolation and estimation of the overall spatial pattern (Belyaeva et al., 2019).

3. Results

3.1. General statistical description

The summary statistics for monthly gamma dose rates measured at 79 sites during the 12 months in China were shown in Fig. 2, and the data was listed in Table S1. The values were range from 60 to 195 nGy h^{-1} with the average of 86.5 nGy h^{-1} (Fig. 1b). However, the data was skewed and heavy-tailed and was not follow a normal distribution because of the high values of skewness. The higher frequencies were observed at the range from 70 to 90 nGy h^{-1}, which accounting for 68.4% of total sites. Three higher values, 195, 179 and 140 nGy h^{-1}, were recorded at the sites of Lhasa, Waliguan and Golmud in Qinghai–Tibet Plateau, respectively. The differences of TGRD among these sites may be results of fluctuation of some local environmental factors, such as the geological factors, meteorological factors and air quality indices.

Table 1
Radiological indices including terrestrial gamma radiation dose rate (TGRD), annual effective dose equivalent (AEDE) and excess lifetime cancer risk (ELCR) in the provinces of China and historical data from 1983 to 1990.

Province	2018				1983–1990
	TGRD (nGy h^{-1})		AEDE (mSv y^{-1})	ELCR (unitless)	TGRD (nGy h^{-1})
	Mean	Range			Range
Beijing	89.4	88.3–90.6	0.110	4.2E – 04	29.2–88.9
Tianjin	72.9	72.3–73.8	0.089	3.4E – 04	36.0–99.7
Hebei	82.8	73.2–75.5	0.102	3.9E – 04	28.0–198.7
Shanxi	85.5	81.6–87.7	0.105	4.0E – 04	31.1–85.7
Inner Mongolia	101.0	81.9–113.7	0.124	4.8E – 04	9.6–186.2
Liaoning	80.1	71.4–101.5	0.098	3.8E – 04	19.8–178.3
Jilin	82.7	68–114.7	0.101	3.9E – 04	18.9–128.6
Heilongjiang	78.9	68.3–88.5	0.097	3.7E – 04	21.6–196.9
Shanghai	75.1	71.4–78.7	0.092	3.5E – 04	34.2–79.5
Jiangsu	69.4	59.3–76.7	0.085	3.3E – 04	33.1–72.6
Zhejiang	84.2	80.2–91	0.103	4.0E – 04	18.6–149.5
Anhui	73.1	67.4–76.5	0.090	3.5E – 04	27.5–132.9
Fujian	107.9	99.1–116.7	0.132	5.1E – 04	25.9–334.3
Jiangxi	81.8	62.5–99.2	0.100	3.9E – 04	13.7–340.8
Shandong	76.5	66–93	0.094	3.6E – 04	16.9–162.6
Henan	75.9	72.2–79	0.093	3.6E – 04	17.5–141.7
Hubei	73.8	68.7–79.6	0.090	3.5E – 04	10.9–140.3
Hunan	78.0	67.5–90.6	0.096	3.7E – 04	21.0–271.2
Guangdong	88.8	76.1–106.3	0.109	4.2E – 04	17.7–193.1
Guangxi	75.0	69–81.3	0.092	3.5E – 04	10.7–238.7
Hainan	63.1	58.1–69	0.077	3.0E – 04	17.7–193.1
Chongqing	79.6	77.7–80.7	0.098	3.8E – 04	2.4–214.0
Sichuan	79.7	69.8–89.7	0.098	3.8E – 04	2.4–214.0
Guizhou	80.1	67.8–94.2	0.098	3.8E – 04	13.1–142.3
Yunnan	81.8	72–87.8	0.100	3.9E – 04	9.9–167.1
Qinghai–Tibet	194.9	193–196.9	0.239	9.2E – 04	24.4–166.0
Shaanxi	84.1	69.2–99.3	0.103	4.0E – 04	25.0–150.0
Gansu	106.3	97.3–116.8	0.130	5.0E – 04	16.9–128.4
Qinghai	140.9	103.6–184.5	0.173	6.7E – 04	24.7–128.0
Ningxia	89.1	86.7–92.9	0.109	4.2E – 04	38.8–87.6
Xinjiang	89.1	69.8–119.6	0.109	4.2E – 04	11.7–326.4
World average	59.0	–[a]	0.07	2.9E – 04	–

[a] "–" not available.

3.2. Mapping and spatial analysis

The map of the TGRD distribution by using the IDW interpolate method was shown in Fig. 3. It was worth noting that the highest dose rate of 195 nGy h^{-1} was measured in Lhasa, and followed the Waliguan (179 nGy h^{-1}) and Golmud (140 nGy h^{-1}), these sites were all located in Qinghai–Tibet Plateau. These are consistent with the results mentioned in general statistical description. The TGRD values above 100 nGy h^{-1} were also recorded at the sites in Inner Mongolia, Northeastern and southeastern China. For other regions, the lower values are range from 60 nGy h^{-1} to 90 nGy h^{-1}, which measured in the Tarim Basin, the central and southern China.

3.3. Radiological indices

In order to estimate the gamma dose rate and associated human health risks, the radiological indices AEDE and ELCR were calculated using the TGRD and other constants and results were listed in Table 1. The results showed that the AEDE values in range of 0.07–0.24 mSv y^{-1}, with the average of 0.11 mSv y^{-1}. The highest value (0.24 mSv y^{-1}) was also obtained from the Qinghai–Tibet Plateau. Most of the values of the ELCR were higher than the world average, 2.9E-04, account for about of 96% monitoring sites. However, these were lower than the limited value of AEDE, 1 mSv, in the national standard, which indicated that the current radiation level was safety for public. Furthermore, the mean level of ELCR in Hainan Island, calculated at 2.7E-04, was comparable to world average. Although values of AEDE and ELCR were higher than world average, the values of TGRD were within the range of background values in 1983–1990 (He et al., 1992). In addition, the radiological index, ELCR is in direct proportion to the TGRD and AEDE based on the analysis of calculating equations. With the above analysis, it can be concluded that radiological indices were also within the acceptable range of values (see Table 1).

3.4. Influencing factors

The q values of 14 potential factors on TGRD were obtained using the geographical detector method, and the results were listed in Tables 2 and 3. As shown in Table 2, the critical environmental factors influenced the TGRD distribution in order of q value were: sunshine duration (0.94), atmosphere pressure (0.87), altitude (0.86), and rainfall (0.83). In addition, these factors had significant difference compared with other factors ($P < 0.001$). However, among the air pollution factors, the main driving factor related to the TGRD was only the CO concentration (0.69) (Table 3). By contrast, the lowest influence factors were wind speed (0.19) and concentrations of gaseous pollutants, such as SO_2 and NO_2 (Tables 2 and 3). Therefore, the environmental factors including meteorological factors and altitude have more impact on TGRD, instead of the air pollution-related factors.

4. Discussion

In this study, the current spatial distribution of TGRD were presented using the geostatistical technology. The results showed the values of TGRD were range from 60 to 195 nGy h^{-1} with the average of 86.5 nGy

Table 2
Results of environmental factors by the geographic detector analysis.

	Rainfall	Atmosphere pressure	Wind speed	Air temperature	Relative humidity	Sunshine duration	Altitude
q	0.83	0.87	0.19	0.64	0.68	0.94	0.86
Atmosphere pressure	N[a]						
Wind speed	Y[b]	Y					
Air temperature	Y	Y	Y				
Relative humidity	Y	Y	Y	N			
Sunshine duration	N	N	Y	Y	Y		
Altitude	N	N	Y	Y	N	N	

[a] N denotes there have no significant difference between two variations.
[b] Y represents there have significant difference between two variations.

Table 3
Results of air pollution factors by the geographic detector analysis.

	AQI	PM2.5	PM10	SO_2	CO	NO_2	O_3
q	0.26	0.23	0.27	0.13	0.69	0.20	0.27
AQI							
PM2.5	N[b]						
PM10	N	N					
SO_2	Y[a]	N	Y				
CO	Y	Y	Y	Y			
NO_2	N	N	N	N	Y		
O_3	N	N	N	Y	Y	N	

[a] Y represents there have significant difference between two variations.
[b] N denotes there have no significant difference between two variations.

h^{-1}, and the higher values were measured in Qingahi-Tibet Plateau. However, these were within the range of previous studies in China (He et al., 1992). Furthermore, the average value of this study is higher than the world average level. The spatial distribution of TGRD are influenced by many environmental factors, as a result, the distribution of TGRD vary from the different region. The TGRD rates in Jos Plateau, Nigeria ranged from 40 to 1265 nGy h^{-1} with a mean value of 250 nGy h^{-1} (Abba et al., 2017), which are higher than in China, even in the Qingahi-Tibet Plateau. In Negeri Sembilan, Malaysia, the values ranged from 71 ± 3 nGy h^{-1} up to 1000 ± 11 nGy h^{-1} with the average of 330 ± 8 nGy h^{-1} (Norbani et al., 2014). However, the records from Saudi, Arabia were 14 and 279 nGy h^{-1} with an average value of 89 nGy h^{-1}, which is close to that in China. Additionally, the current assessing method of health risk is still limited for the TGRD, the further study should be focus on developing the novel assessment model for multi-pathway exposure based on the related results of toxicological or physiological studies.

The higher values of TGRD in the Qingahi−Tibet Plateau may be the results of the specific environmental types. In this study, the results of geographic detector showed that the sunshine duration, atmosphere pressure, altitude, and rainfall were driving factors of the TGRD in the region (Table 2 and Fig. 4). In fact, the altitude could significantly impact the weather and climate condition, such as the pressure, sunshine duration and precipitation (Cui et al., 2008).

It is generally known that the Qinghai−Tibet Plateau, at an average elevation of above 4000 m, belonging to the typical plateau continental climate such as drying, less air dense, long sunshine hours, which may enhance transmittance of the atmospheric layer and increase the radiation by ionization of cosmic rays come from space (Ma et al., 2008; Li et al., 2011). In addition, the higher TGRD value may be caused by the rock layers that composed of volcanic and granitic rocks (Zhao et al., 2015). The study reported that greatest TGRD originating from igneous rock of granitic formations, while the minimum value of TGRD was observed in an area covered by limestone composed of calcite mineral (Norbani et al., 2014). The higher value of TGRD above 100 nGy h^{-1} recorded in southeastern and southern China, which may also be caused by distribution of granitic rock layer (Yan et al., 2018; Zhao et al., 2018). Similarly, the high values of TGRD were also recorded by previous

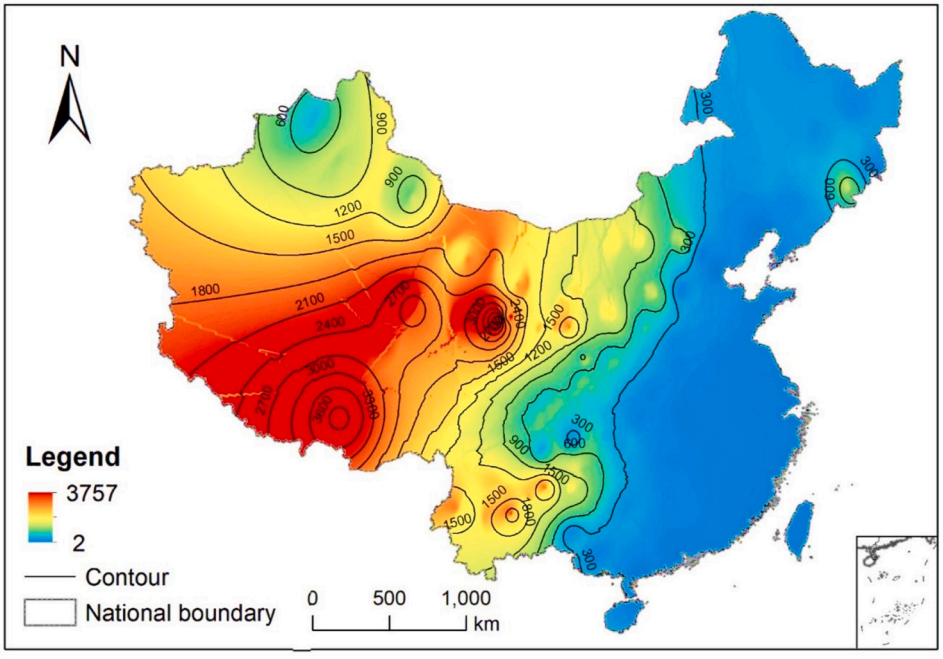

Fig. 4. Contour map based on the data of monitoring sites in China by using the distance inverse weight (IDW) interpolate method.

studies in Pakistan and France, because of the cosmic radiation dose rates varied with altitude and solar activity (Billon et al., 2005; Jabbar et al., 2008). Additionally, many studies had reported the impacts of geological type and soil type on the TGRD (Ramli, 1997; Garba et al., 2014; Belyaeva et al., 2019). Therefore, the distribution of TGRD in China is the results of radionuclides in typical rock, ionization of cosmic rays, and impacts of the dominant meteorological factors.

We found that meteorological factors and altitude have more impact on TGRD than the air pollution-related factors, which was mainly based on calculating the q value using the method of factor detector. The q values of meteorological factors were higher than those of air pollutants and quality indices (Table 2). Many previous studies verified the rainfall and snowfall, altitude had important effects on the distribution of TGRD (Billon et al., 2005; Inomata et al., 2007; Jabbar et al., 2008). For example, strong precipitation intensity effectively removes aerosols and Rn-222 progeny from the atmosphere and consequently, extraordinarily high Δγ ray dose rates would occur (Inomata et al., 2007; Hirose et al., 1993). To date, the report about the influence of air pollutant and quality indices on the environmental radiation are still limited. Further studies are needed for the relationships between environmental radiation and air pollutants and the quality indices on regional and global scale. Our results provide useful information on studying the influence mechanism of the TGRD distribution and on the variability of the natural terrestrial gamma radiation in China and exposure data for risk assessment from low dose chronic exposures.

5. Conclusions

In this study, the current spatial distribution and the risk assessment of terrestrial gamma radiation dose (TGRD) in China were investigated by using spatial interpolation based on the multiple data released in 2018. The driving factors influence on the TGRD distribution were also identified by using the geographic detector. The results showed that the values of TGRD are range from 60 to 195 nGy h^{-1} with the average of 86.5 nGy h^{-1}, and the higher values were recorded in Qingahi–Tibet Plateau. Most of values of AEDE and ELCR were higher than the world average, but these were all within the range of background value in China. The factors of sunshine duration (0.94), atmosphere pressure (0.87), altitude (0.86), and rainfall (0.83) have a significant impact on the TGRD distribution. Furthermore, meteorological factors and altitude have more impact on TGRD than the air pollution-related factors. The findings of our study can fill the gap of the study on driving mechanisms of TGRD to a certain extent, and provide a theoretical basis for the further study on evaluating the natural radioactivity.

Declaration of competing interest

The authors declare that they have no known competing financial interests or personal relationships that could have appeared to influence the work reported in this paper.

Acknowledgments

This work was supported by Key R & D and Promotion Projects of Henan Province, China (Grant No. 202102310268 and No. 182102311110), the Scientific Research Foundation for High-level Professionals of Zhoukou Normal University, China (Grant No. ZKUNC2019006), and the Opening Project of Henan Province Key Laboratory of Water Pollution Control and Rehabilitation Technology (Grant No. CJSZ2018004).

Appendix B. Supplementary data

Supplementary data to this article can be found online at https://doi.org/10.1016/j.jenvrad.2020.106325.

References

Abba, H.T., Hassan, W.M.S.W., Saleh, M.A., Aliyu, A.S., Ramli, A.T., 2017. Terrestrial gamma radiation dose (TGRD) levels in northern zone of Jos Plateau, Nigeria: statistical relationship between dose rates and geological formations. Radiat. Phys. Chem. 140, 167–172.

Alazemi, N., Bajoga, A.D., Bradley, D.A., Regan, P.H., Shams, H., 2016. Soil radioactivity levels, radiological maps and risk assessment for the state of Kuwait. Chemosphere 154, 55–62.

Al-Ghorabie, F.H.H., 2005. Measurements of environmental terrestrial gamma radiation dose rate in three mountainous locations in the western region of Saudi Arabia. Environ. Res. 98 (2), 160–166.

Alomari, A.H., Saleh, M.A., Hashim, S., Alsayaheen, A., 2019. Investigation of natural gamma radiation dose rate (GDR) levels and its relationship with soil type and underlying geological formations in Jordan. J. Afr. Earth Sci. 155, 32–42.

Bai, L., Jiang, L., Yang, D., Liu, Y., 2019. Quantifying the spatial heterogeneity influences of natural and socioeconomic factors and their interactions on air pollution using the geographical detector method: a case study of the Yangtze River Economic Belt, China. J. Clean. Prod. 232, 692–704.

Belyaeva, O., Pyuskyulyan, K., Movsisyan, N., Saghatelyan, A., Carvalho, F.P., 2019. Natural radioactivity in urban soils of mining centers in Armenia: dose rate and risk assessment. Chemosphere 225, 859–870.

Billon, S., Morin, A., Caër, S., Baysson, H., Gambard, J.P., Backe, J.C., Rannou, A., Tirmarche, M., Laurier, D., 2005. French population exposure to radon, terrestrial gamma and cosmic rays. Radiat. Protect. Dosim. 113 (3), 314–320.

CMA, 2018. Ground meteorological data, 2020-02-26. http://data.cma.cn/data/index/6d1b5efbdcbf9a58.html.

CNEMC, 2018. National real time air quality, 2020-02-21. http://www.cnemc.cn/.

Cui, X., Gu, S., Zhao, X., Wu, J., Kato, T., Tang, Y., 2008. Diurnal and seasonal variations of UV radiation on the northern edge of the Qinghai-Tibetan Plateau. Agric. For. Meteorol. 148 (1), 144–151.

El Zrelli, R., Rabaoui, L., van Beek, P., Castet, S., Souhaut, M., Grégoire, M., Courjault-Radé, P., 2019. Natural radioactivity and radiation hazard assessment of industrial wastes from the coastal phosphate treatment plants of Gabes (Tunisia, Southern Mediterranean Sea). Mar. Pollut. Bull. 146, 454–461.

Feng, W., Guo, Z., Peng, C., Xiao, X., Shi, L., Zeng, P., Ran, H., Xue, Q., 2019a. Atmospheric bulk deposition of heavy metal(loid)s in central south China: fluxes, influencing factors and implication for paddy soils. J. Hazard Mater. 371, 634–642.

Feng, W., Guo, Z., Xiao, X., Peng, C., Shi, L., Ran, H., Xu, W., 2019b. Atmospheric deposition as a source of cadmium and lead to soil-rice system and associated risk assessment. Ecotox. Environ. Safe. 180, 160–167.

Garba, N.N., Ramli, A.T., Saleh, M.A., Sanusi, M.S., Gabdo, H.T., 2014. Assessment of terrestrial gamma radiation dose rate (TGRD) of Kelantan State, Malaysia: relationship between the geological formation and soil type to radiation dose rate. J. Radioanal. Nucl. Chem. 302 (1), 201–209.

He, Z., Luo, G., Huang, J., 1992. Nationwide survey of environmental natural radioactivity level in China. Radiat. Prot. 12 (2), 81–95.

Hirose, K., Takatani, S., Aoyama, M., 1993. Wet deposition of radionuclides derived from the Chernobyl accident. J. Atmos. Chem. 17 (1), 61–71.

ICRP, 2008. Radiation dose to patients from radiopharmaceuticals. Addendum 3 to ICRP publication 53. ICRP publication 106. Approved by the commission in october 2007. Ann. ICRP 38 (1–2), 1.

Inomata, Y., Chiba, M., Igarashi, Y., Aoyama, M., Hirose, K., 2007. Seasonal and spatial variations of enhanced gamma ray dose rates derived from ^{222}Rn progeny during precipitation in Japan. Atmos. Environ. 41 (37), 8043–8057.

Jabbar, T., Khan, K., Subhani, M.S., Akhter, P., Jabbar, A., 2008. Environmental gamma radiation measurement in District Swat, Pakistan. Radiat. Protect. Dosim. 132 (1), 88–93.

Jibiri, N.N., 2001. Assessment of health risk levels associated with terrestrial gamma radiation dose rates in Nigeria. Environ. Int. 27 (1), 21–26.

Kuang, W., Li, Z., Hamdi, R., 2020. Comparison of surface radiation and turbulent heat fluxes in Olympic Forest Park and on a building roof in Beijing, China. Urban Climate 31, 100562.

Kumara, P.A.R.P., Mahakumara, P., Jayalath, A., Jayalath, C.P., 2018. Estimating natural radiation exposure from building materials used in Sri Lanka. Journal of Radiation Research and Applied Sciences 11 (4), 350–354.

Li, H., Ma, W., Lian, Y., Wang, X., Zhao, L., 2011. Global solar radiation estimation with sunshine duration in Tibet, China. Renew. Energy 36 (11), 3141–3145.

Lu, X., Chao, S., Yang, F., 2014. Determination of natural radioactivity and associated radiation hazard in building materials used in Weinan, China. Radiat. Phys. Chem. 99, 62–67.

Luo, W., Jasiewicz, J., Stepinski, T., Wang, J., Xu, C., Cang, X., 2016. Spatial association between dissection density and environmental factors over the entire conterminous United States. Geophys. Res. Lett. 43 (2), 692–700.

Ma, Y., Kang, S., Zhu, L., Xu, B., Yao, T., 2008. Roof of the World: Tibetan observation and research platform. Bull. Am. Meteorol. Soc. 89, 1487.

Manohar, S.N., Meijer, H.A.J., Herber, M.A., 2013. Radon flux maps for The Netherlands and Europe using terrestrial gamma radiation derived from soil radionuclides. Atmos. Environ. 81, 399–412.

MEP, 2018. List of monitoring reports. http://data.rmtc.org.cn:8080/gis/DocfileList.html, 2020-03-21.

Mercier, J.F., Tracy, B.L., D'Amours, R., Chagnon, F., Hoffman, I., Korpach, E.P., Johnson, S., Ungar, R.K., 2009. Increased environmental gamma-ray dose rate during precipitation: a strong correlation with contributing air mass. J. Environ. Radioact. 100, 527–533.

Momčilović, M., Kovačević, J., Dragović, S., 2010. Population doses from terrestrial exposure in the vicinity of abandoned uranium mines in Serbia. Radiat. Meas. 45 (2), 225–230.
Monica, S., Prasad, A.K.V., Soniya, S.R., Jojo, J., 2019. Comparison of gamma dose levels in assessed by various methods. Mater. Today Proc 16, 776–783.
Nishikawa, T., Tamagawa, Y., Aoki, M., Okabe, S., 1995. Analysis of the time variation of environmental gamma radiation due to the precipitation. Appl. Radiat. Isot. 46, 603–604.
Norbani, N.E., Abdullah Salim, N.A., Saat, A., Hamzah, Z., Ramli, A.T., Wan Idris, W.M. R., Jaafar, M.Z., Bradley, D.A., Abdul Rahman, A.T., 2014. Terrestrial gamma radiation dose rates (TGRD) from surface soil in Negeri Sembilan, Malaysia. Radiat. Phys. Chem. 104, 112–117.
NHC, 2019. Statistical bulletin on the development of health services of China in 2018. http://www.nhc.gov.cn/guihuaxxs/s10748/201905/9b8d52727cf346049de8acce25ffcbd0.shtml. 2019-05-22.
Ouakarrouch, M., El Azhary, K., Laaroussi, N., Garoum, M., Feiz, A., 2019. Three-dimensional numerical simulation of conduction, natural convection, and radiation through alveolar building walls. Case Studies in Construction Materials 11, e249.
Ramli, A.T., 1997. Environmental terrestrial gamma radiation dose and its relationship with soil type and underlying geological formations in Pontian District, Malaysia. Appl. Radiat. Isot. 48 (3), 407–412.
Ravisankar, R., Raghu, Y., Chandrasekaran, A., Suresh Gandhi, M., Vijayagopal, P., Venkatraman, B., 2016. Determination of natural radioactivity and the associated radiation hazards in building materials used in Polur, Tiruvannamalai District, Tamilnadu, India using gamma ray spectrometry with statistical approach. J. Geochem. Explor. 163, 41–52.
Ren, Y., Deng, L., Zuo, S., Luo, Y., Shao, G., Wei, X., Hua, L., Yang, Y., 2014. Geographical modeling of spatial interaction between human activity and forest connectivity in an urban landscape of southeast China. Landsc. Ecol. 29 (10), 1741–1758.
Sanusi, M.S.M., Ramli, A.T., Gabdo, H.T., Garba, N.N., Heryanshah, A., Wagiran, H., Said, M.N., 2014. Isodose mapping of terrestrial gamma radiation dose rate of Selangor state, Kuala Lumpur and Putrajaya, Malaysia. J. Environ. Radioact. 135, 67–74.
SEPA, 1993. Norm for the Measurement of Environmental Terrestrial Gamma-Radiation Dose Rate, GB/T 14583-93. China Standard Press, pp. 1–5.
Sethy, N.K., Jha, V.N., Sutar, A.K., Rath, P., Sahoo, S.K., Ravi, P.M., Tripathi, R.M., 2014. Assessment of naturally occurring radioactive materials in the surface soil of uranium mining area of Jharkhand, India. J. Geochem. Explor. 142, 29–35.
Sharma, P., Kumar Meher, P., Prasad Mishra, K., 2014. Terrestrial gamma radiation dose measurement and health hazard along river Alaknanda and Ganges in India. Journal of Radiation Research and Applied Sciences 7 (4), 595–600.
Smetsers, R.C.G.M., Tomas, J.M., 2019. A practical approach to limit the radiation dose from building materials applied in dwellings, in compliance with the Euratom Basic Safety Standards. J. Environ. Radioact. 196, 40–49.
Szabó, K.Z., Jordan, G., Petrik, A., Horváth, Á., Szabó, C., 2017. Spatial analysis of ambient gamma dose equivalent rate data by means of digital image processing techniques. J. Environ. Radioact. 166, 309–320.
Taskin, H., Karavus, M., Ay, P., Topuzoglu, A., Hidiroglu, S., Karahan, G., 2009. Radionuclide concentrations in soil and lifetime cancer risk due to gamma radioactivity in Kirklareli, Turkey. J. Environ. Radioact. 100 (1), 49–53.
Torres, S.B., Petrik, A., Szabó, K.Z., Jordan, G., Yao, J., Szabó, C., 2018. Spatial relationship between the field-measured ambient gamma dose equivalent rate and geological conditions in a granitic area, Velence Hills, Hungary: an application of digital spatial analysis methods. J. Environ. Radioact. 192, 267–278.
Tufail, M., Akhtar, N., Waqas, M., 2006. Measurement of terrestrial radiation for assessment of gamma dose from cultivated and barren saline soils of Faisalabad in Pakistan. Radiat. Meas. 41 (4), 443–451.
UNSCEAR, 2000. Sources and Effects of Ionizing Radiations. United Nations Scientific Committee on the Effects of Atomic Radiation, New York, USA.
Wang, J., Hu, Y., 2012. Environmental health risk detection with GeogDetector. Environ. Model. Software 33, 114–115.
Wang, J., Zhang, T., Fu, B., 2016. A measure of spatial stratified heterogeneity. Ecol. Indicat. 67, 250–256.
Wang, J.F., Li, X.H., Christakos, G., Liao, Y.L., Zhang, T., Gu, X., Zheng, X.Y., 2010. Geographical detectors-based health risk assessment and its application in the neural tube defects study of the heshun region, China. Int. J. Geogr. Inf. Sci. 24 (1), 107–127.
Wei, W., Guo, Z., Zhou, L., Xie, B., Zhou, J., 2020. Assessing environmental interference in northern China using a spatial distance model: from the perspective of geographic detection. Sci. Total Environ. 709, 136170.
Yan, Q., Wang, H., Qiu, Z., Wei, X., Li, P., Dong, R., Zhang, X., Zhou, K., 2018. Origin of Early Cretaceous A-type granite and related Sn mineralization in the Sanjiaowo deposit, eastern Guangdong, SE China and its tectonic implication. Ore Geol. Rev. 93, 60–80.
Yakovleva, V.S., Nagorsky, P.M., Cherepnev, M.S., Kondratyeva, A.G., Ryabkina, K.S., 2016. Effect of precipitation on the background levels of the atmospheric β- and γ-radiation. Appl. Radiat. Isot. 118, 190–195.
Yeşilkanat, C.M., Kobya, Y., Taşkın, H., Çevik, U., 2017. Spatial interpolation and radiological mapping of ambient gamma dose rate by using artificial neural networks and fuzzy logic methods. J. Environ. Radioact. 175–176, 78–93.
Zhang, X., Xu, C., Xiao, G., 2020. Spatial heterogeneity of the association between temperature and hand, foot, and mouth disease risk in metropolitan and other areas. Sci. Total Environ. 713, 136623.
Zhao, S.Q., Tan, J., Wei, J.H., Tian, N., Zhang, D.H., Liang, S.N., Chen, J.J., 2015. Late Triassic Batang Group arc volcanic rocks in the northeastern margin of Qiangtang terrane, northern Tibet: partial melting of juvenile crust and implications for Paleo-Tethys ocean subduction. Int. J. Earth Sci. 104 (2), 369–387.
Zhao, X., Jiang, Y., Yu, S., Xing, G., Yu, M., Liu, Y., 2018. Geochemical, zircon U–Pb–Hf, and whole-rock Sr–Nd isotopic study of Late Jurassic Sanming A-type granite in the Wuyi area, Fujian province, Southeast China. Geol. J. 53 (5), 2204–2218.